Supporting Information for

Dealloyed Intra-Nanogap Particles with Highly Robust, Quantifiable Surface-Enhanced Raman Scattering Signals for Biosensing and Bioimaging Applications

Minho Kim, Sung Min Ko, Jae-Myoung Kim, Jiwoong Son, Chungyeon Lee, Won-Kyu Rhim, and Jwa-Min Nam*

Department of Chemistry, Seoul National University, Seoul 08826, South Korea

*E-mail: jmnam@snu.ac.kr

Experimental Methods

Reagents and materials

Gold nanoparticles (AuNPs, average diameter of 40 nm) and magnetic microparticles (MMPs, Dynabeads® MyOne™ Carboxylic Acid, average diameter of 1 μm) were purchased from Ted Pella, Inc. (Redding, CA, USA) and Invitrogen Dynal AS (Oslo, Norway), respectively. HPLC-purified oligonucleotides were purchased from Bioneer (Daejeon, South Korea) and carboxymethyl-PEG-thiol (CM-PEG-SH, M_w≈5000) was purchased from Laysan Bio, Inc. (Arab, AL, USA). Cyclo(Arg-Gly-Asp-D-Phe-Lys) (c(RGDyK), cRGD) peptide was purchased from Peptides International, Inc. (Louisville, KY, USA). Gold(III) chloride trihydrate ($HAuCl_4 \cdot 3H_2O$, ≥99.9%), silver nitrate ($AgNO_3$, 99.9999%), 4-mercaptopyridine (4-MPy, 95%), polyvinylpyrrolidone (PVP, M_w≈40000), ammonium hydroxide solution (NH_4OH, 28.0-30.0% NH_3 basis), L-ascorbic acid (AA, ≥99.0%), iron(III) nitrate nonahydrate ($Fe(NO_3)_3 \cdot 9H_2O$, ≥98.0%), 2-(*N*-morpholino)ethanesulfonic acid (MES, ≥99.0%), *N*-(3-dimethylaminopropyl)-*N'*-ethylcarbodiimide hydrochloride (EDC, commercial grade), *N*-hydroxysulfosuccinimide sodium salt (Sulfo-NHS, ≥98%), ethylenediaminetetraacetic acid (EDTA, 99.4-100.06%), DL-dithiothreitol (DTT, ≥99.0%), Tween®-20, and sodium dodecyl sulfate (SDS, ≥98.5%) were purchased from Sigma-Aldrich (St. Louis, MO, USA). Tris[hydroxymethyl]aminomethane (Tris, 99.8-100.1%) was purchased from USB Corporation (Cleveland, OH, USA). Ethyl alcohol (anhydrous, 99.9%) and sodium chloride (NaCl, ≥99.0%) were purchased from DAEJUNG Chemicals & Metals Co. (Siheung, Gyeonggi, Korea). All the chemical reagents were used as received without further purification. NANOpure water (Millipore, Milli-Q 18.2 MΩ·cm) was used throughout the experiments.

Preparation of 4-MPy-modified Au nanoparticles

To attach the Raman reporter molecules (4-mercaptopyridine, 4-MPy) onto the AuNPs, 10 μL of an ethanol solution of 4-MPy (1 mM) was injected into 1 mL of a solution (100 pM) of the Au NPs (average diameter of 40 nm). The resulting mixture was then shaken over 2 h. Next, the 4-MPy-modified AuNPs (MPy-AuNPs) were washed with distilled water by centrifugation at 6000 rpm for 10 min and redispersed in distilled water for further use.

Synthesis of Au/Au-Ag core/alloy shell nanoparticles

The Au/Au-Ag core/alloy shell NPs (CAS NPs) were synthesized using a previously reported procedure with minor modifications.[1] Typically, 200 μL of the MPy-AuNPs solution (100 pM) and 200 μL of a polyvinylpyrrolidone (PVP, $M_w \approx 40000$) solution (1 wt%) were mixed gently. Then, 50 μL of a $AgNO_3$ solution (1 mM), 16 μL of a NH_4OH solution, and 150 μL of a $HAuCl_4$ solution (1 mM) were sequentially

added to the mixture. Next, 200 μL of an L-ascorbic acid (AA) solution (20 mM) was immediately injected into the mixture under gentle shaking. The resulting mixture was shaken gently for 1 h at room temperature. Finally, the solution was washed twice with distilled water by centrifugation at 6000 rpm for 10 min and redispersed in distilled water.

Synthesis of gap-less Au/Au core/shell nanoparticles

To synthesize the gap-less Au/Au core/shell NPs (gap-less AuNPs), we simply modified the procedure for synthesising the CAS NPs. Typically, 200 μL of the $HAuCl_4$ solution (1 mM) was added instead of 50 μL of the $AgNO_3$ (1 mM) solution and 150 μL of the $HAuCl_4$ solution (1 mM) during the synthesis process. The rest of the procedure was the same as that for the synthesis of the CAS NPs.

Synthesis of Au-Ag dealloyed intra-nanogap particles

The Au-Ag dealloyed intra-nanogap particles (DIPs) were synthesized by introducing $Fe(NO_3)_3$ as a Ag etchant into the fabricated CAS NPs. Typically, 100 μL of a solution of the CAS NPs (100 pM) was mixed with 100 μL of a PVP solution (1 wt%). Next, 125 μL of an $Fe(NO_3)_3$ solution (20 mM) was injected into this mixture under gentle shaking. The resulting mixture was shaken mildly for 30 min at room temperature, washed twice with distilled water by centrifugation at 6000 rpm for 10 min, and redispersed in distilled water.

Setup for micro-Raman spectroscopy

For the solution-state Raman analysis, a solution of the as-synthesized NPs (100 pM) was loaded into a capillary tube (soda lime glass; CAT. NO: 2502) obtained from Kimble Chase (Vineland, NJ, USA). All the Raman measurements were performed using a Renishaw inVia microscope equipped with 514 (5 mW), 633 (4 mW), and 785 nm (4 mW) excitation lasers, a 20× objective lens (NA = 0.40, Leica), and a standard charge-coupled device (CCD) array detector (576 × 384 pixels; Peltier; cooled to -70 °C). The SERS spectra were acquired using an acquisition period of 10 s and were recorded for wavenumbers of 800–1800 cm^{-1}.

Setup for AFM-correlated Raman spectroscopy

To obtain the SERS spectra from the individual NPs, we employed an AFM-correlated Raman microscope (Ntegra, NT-MDT) equipped with an inverted optical microscope (IX 73, Olympus). We performed the AFM-based multistep tip-matching procedure based on previous studies, in order to accurately match the end of the AFM tip and the laser focal spot.[2,3] First, the laser beam was focused on the upper surface of a particle-loaded cover glass slip (poly-L-lysine-coated cover glass), and end of the AFM tip was positioned on the laser focal spot, which was observed with micrometer-level accuracy using a video camera. Next, Rayleigh scattering images were recorded during the scanning of the tip along the x- and y-axes, and the AFM tip was subsequently

moved to the region with the highest scattering intensity, such that the tip was located on the laser focal spot. Finally, the end of the AFM tip was moved with nanometer-level precision by observing the intensity of the Raman signal of the silicon (520 cm^{-1}) in the AFM tip. The highest Raman signal intensity was obtained when the end of the AFM tip was located exactly at the center of the laser focal spot. In this tip-matching state, Rayleigh scattering images and AFM topographical images were obtained simultaneously using a piezoelectric x, y sample scanner. The SERS spectra of the individual NPs were obtained using a CCD detector (1024 × 256 pixels; Peltier; cooled to -70 °C, Andor) and a 633 nm excitation laser (He-Ne laser, Thorlabs). The exposure time was 20 s, and the laser power was 60 μW. An oil-immersed microscope objective (100×, NA = 1.4, Olympus) was used to focus the laser beam on a diffraction-limited spot (~ 250 nm when a 633 nm laser was used).

Theoretical calculations

The extinction spectra of the NPs were calculated using Mie theory.[4] An analytic model[5] was used for the dielectric functions of Au and Au-Ag alloy. The particles were considered as embedded in water ($\varepsilon = 1.33^2$). The average particle sizes, interior-nanogap sizes, shell thicknesses, and atomic compositions of the as-synthesized NPs are given in Figure S1 and Table S1. We used Smith's method[6] for effective dielectric function of the interior-nanogap region of DIP, and the interior-nanogap region was modeled as a mixture of gold and water. For metal-rich mixtures, an average unit within the interior nanogap was considered as spherical dielectric inclusion surrounded by spherical shell of the metal. The effective dielectric function is the value that does not alter the electric field under replacement the unit structure with homogeneous effective medium. This model mostly targets metal-rich mixtures but also applicable to dielectric-rich mixtures whose metallic parts are connected to each other and overall behavior is conductive. Our structure is the case because the mixture within interior-nanogap is of thin shell form and squeezed between metallic core and shell and each inclusion can be conductive.

Calculations of SERS enhancement factor

The SERS enhancement factor (EF) was calculated using the following equation (Equation 1):

$$\text{Enhancement factor (EF)} = \frac{I_{SERS}}{N_{SERS}} \Big/ \frac{I_{BULK}}{N_{BULK}} \qquad (1)$$

where I_{SERS} and I_{BULK} are the intensities of the Raman peak at 1003 cm^{-1} for the individual DIP and the pure 4-MPy solution (200 mM, 22.23 mg/mL), respectively; and N_{SERS} and N_{BULK} are the number of 4-MPy molecules on a single DIP and within solution, respectively. The number of 4-MPy molecules on a single DIP (N_{SERS}) was estimated by assuming that the maximum number of 4-MPy molecules were packed on the AuNPs (average diameter of 40 nm); the average monomolecular area of 4-MPy has been estimated to be 0.18 nm^2.[7,8]

To estimate I_{BULK} and N_{BULK}, 12 μL of a 4-MPy solution (200 mM, 22.23 mg/mL) was introduced into a sticker chamber placed on a glass substrate and illuminated with a 633 nm laser for 30 s through an objective lens (20×, NA = 0.4). Assuming that the effective excitation volume (V_{BULK}) was a cylinder, the height (h) was calculated using the following equation (Equation 2):

$$\frac{h}{2r} = \frac{3.28\eta}{NA} \qquad (2)$$

where η is the refractive index of the medium (water; 1.33) and r is the radius of the laser beam (5 μm). Further, N_{BULK} was calculated using the following equation (Equation 3):

$$N_{BULK} = (V_{BULK} \text{ x } D/M) \text{ x } N_A \qquad (3)$$

where D is the density of 4-MPy (22.23 mg/mL), M is the molar mass of 4-MPy (111.16 g/mol), and N_A is Avogadro's constant (6.02×10^{23} mol^{-1}). Lastly, we measured and plotted the incident-laser-power-dependent Raman intensities of the 4-MPy solution to determine the value of I_{BULK} for calculating the SERS EF (Figure S9).

Preparation of DNA-modified magnetic microparticles

We prepared DNA-modified magnetic microparticles (DNA-MMPs) according to the company's instruction (Invitrogen Dynal AS) with minor modifications. Typically, 200 μL of a solution of the MMPs coated with the carboxyl functional group (10 mg/mL) was transferred to a tube and placed in a magnetic separator to remove the supernatant. After the supernatant had been discarded, the MMPs were washed twice with 200 μL of 100 mM MES buffer (pH 4.8) and redispersed in 20 μL of the MES buffer. Next, 10 μL of 5'-amine-modified oligonucleotides (1 mM, DNA sequence: 5'-NH_2-A_{10}-PEG_6-AGAAAGAGGAGTTAA-3') and 10 μL of a 1 M EDC solution in the MES buffer (100 mM, pH 4.8) were added to the washed MMPs, and the resulting mixture was shaken for 4 h at room temperature. Finally, the mixture was washed three times with 200 μL of a washing buffer (250 mM, Tris pH 8.0, 0.01% Tween®-20), and the DNA-modified MMPs were suspended in 200 μL of a storage buffer (10 mM, Tris pH 8.0, 1 mM EDTA).

Preparation of DNA-modified DIP Raman probes

To prepare the DNA-modified DIP Raman probes (DIP probes), thiolated oligonucleotides were attached onto the DIPs through Au-S bonding. First, disulfide-modified oligonucleotides were reduced in a 100 mM DTT solution for 2 h at room temperature and purified using an NAP-5 column (Sephadex™ G-25 DNA Grade, GE Healthcare, UK) to obtain thiolated oligonucleotides. Then, the freshly DTT-reduced thiolated oligonucleotides (DNA sequence: 5'-TCCATGCAACTCTAA-A_{10}-SH-3') were added to a solution of the

DIPs and allowed to incubation overnight at room temperature under mild shaking. The solution was then adjusted to obtain a final phosphate concentration of 10 mM (pH 7.4) and a SDS concentration of 0.1% (wt/vol). After incubation for 1 h, the mixture was brought to 0.3 M NaCl by the gradual addition of six aliquots of a 2 M NaCl solution at intervals of 1 h. The mixture was then kept overnight at room temperature under mild shaking. Next, the mixture was washed three times with an assay buffer (10 mM phosphate buffer, 0.3 M NaCl, 0.01% SDS, pH 7.4) by centrifugation at 6000 rpm for 5 min and redispersed in the assay buffer for use as a DNA detection assay.

SERS-based DNA detection assay

The SERS-based DNA detection assays were performed using a typical sandwich-hybridization assay. First, a solution of the target DNA (hepatitis A virus; HAV, DNA sequence: 5'-TTAGAGTTGCATGGATTAACTCCTCTTTCT-3') was serially diluted from 10 aM to 1 pM using an assay buffer (10 mM phosphate buffer, 0.3 M NaCl, 0.01% SDS, pH 7.4); noncomplementary DNA (hepatitis B virus; HBV, DNA sequence: 5'-TTGGCTTTCAGTTATATGGATGATGTGGTA-3') was also used, in order to confirm the DNA targeting specificity of the probes. Next, 100 μL of the diluted target DNA solution was mixed with 1 μL of the DNA-MMP (10 mg/mL) solution, and the mixture was allowed to incubation for 1 h at room temperature under shaking. Then, 20 μL of the DIP probe solution (100 pM) was added to the target-DNA-capturing MMP solution, and the mixture was allowed to incubation for 30 min at room temperature under shaking. The target-captured DIP probe-MMP complexes were washed three times with an assay buffer and the final solution volume was adjusted to 10 μL. For the Raman measurements, 5 μL of this concentrated solution was transferred onto a cover glass placed on a magnet. Owing to the applied magnetic force, the complexes were collected on the surface of the cover glass. The remaining solvent was wiped with tissue paper, and the collected complexes were dried under ambient conditions for use in the Raman measurements. For reducing the variance in the unevenness of the focal spot of the prepared sample, the dried cover glass was inverted (turned upside down), and the focus was adjusted on the backside of the sample. All the Raman measurements were performed using a Renishaw inVia microscopy system with a 785 nm excitation laser (2 mW). The SERS spectra were acquired using an acquisition time of 5 s. For clear identification, the SERS intensities were obtained by consecutive accumulation of five measurements.

Preparation of cRGD peptide-modified DIP imaging probes

To perform SERS-based target-specific cell imaging, the surfaces of the DIPs were functionalized with cRGD peptide, which has a high affinity for integrin $\alpha_v\beta_3$. To prepare the PEGlyated DIPs, first, 50 μL of a 0.5 mM solution of CM-PEG-SH ($M_w \approx 5000$) was added to 500 μL of a dispersion of the DIPs (50 pM) in 0.01% SDS, and the mixture was allowed to rest overnight at room temperature under mild shaking. The mixture was then washed twice with a 50 mM MES buffer solution (pH 4.8) by centrifugation at 6000 rpm for 5 min. Next, the

carboxylic acid part of the PEG attached onto the DIPs was linked with the cRGD peptide through an EDC/Sulfo-NHS coupling reaction. Typically, 25 μL of freshly prepared 20 mM EDC and Sulfo-NHS solutions were sequentially added to 500 μL of the as-prepared PEGlyated DIPs (25 pM) and the reaction mixture was stirred for 20 min. The resulting mixture was then washed twice with a 10 mM phosphate buffer (pH 7.4) by centrifugation at 6000 rpm for 5 min, and the supernatant was discarded. To this concentrated solution, 125 μL of the cRGD peptide (1 mM) dissolved in a 10 mM phosphate buffer (pH 7.4) was added, and the reaction mixture was shaken for 6 h. It was then washed twice with a 10 mM phosphate buffer (pH 7.4) by centrifugation at 6000 rpm for 5 min and suspended in phosphate buffered saline (10 mM phosphate buffer, 0.15 M NaCl, pH 7.4) for further use.

SERS-based target-specific cell imaging

The human malignant U87MG glioma cell line and human breast carcinoma MCF-7 cell line were obtained from American Type Culture Collection (ATCC) and were cultured in Minimum Essential Medium (MEM) and Dulbecco's Modified Eagle Medium (DMEM) along with 10% foetal bovine serum, 100 U/mL penicillin, and 100 μg/mL streptomycin at 37 °C under 5% CO_2. Both types of cells were harvested by trypsin/EDTA, loaded (5×10^3 cells/mL) onto poly-d-lysine-coated 50-mm glass-bottom dishes (MatTek Corporation, Ashland, MA, USA), and incubated overnight. Then, the cell-loaded dishes were rinsed with PBS buffer (10 mM phosphate buffer, 0.15 M NaCl, pH 7.4), filled with the cRGD-functionalized DIPs suspended in a medium (12.5 pM), and kept for 6 h at 37 °C under 5% CO_2. After incubation, the cell monolayer was washed with PBS buffer and fixed with 4% paraformaldehyde. To perform SERS-based target-specific cell imaging, the cells incubated with the cRGD-functionalized DIPs were scanned, and the SERS spectrum at each mapping pixel (2 μm × 2 μm) was recorded. All the Raman measurements were performed using a Renishaw inVia microscopy system with a 785 nm (4 mW) or 633 nm (400 μW) excitation laser, and the SERS signals were recorded for an acquisition time of 1 s for each mapping pixel. Finally, the integrated SERS intensities (from 983 cm^{-1} to 1023 cm^{-1}) for each mapping pixel were color-scaled for cell imaging.

Characterization

The morphological characteristics of the as-synthesized NPs and the target-DNA-induced sandwich hybridization complexes were evaluated using a TEM system (JEM-2100, JEOL), a high-resolution TEM (HR-TEM) system (JEM-2100F, JEOL), and a field-emission SEM (FE-SEM) system (JSM-7800F Prime, JEOL). The elemental maps and line scan profiles of the NPs were obtained using a EDX system (INCA, Oxford Instruments) coupled with an HR-TEM system. The UV-vis spectra were acquired using an UV-vis spectrophotometer (HP 8453, Agilent Technologies).

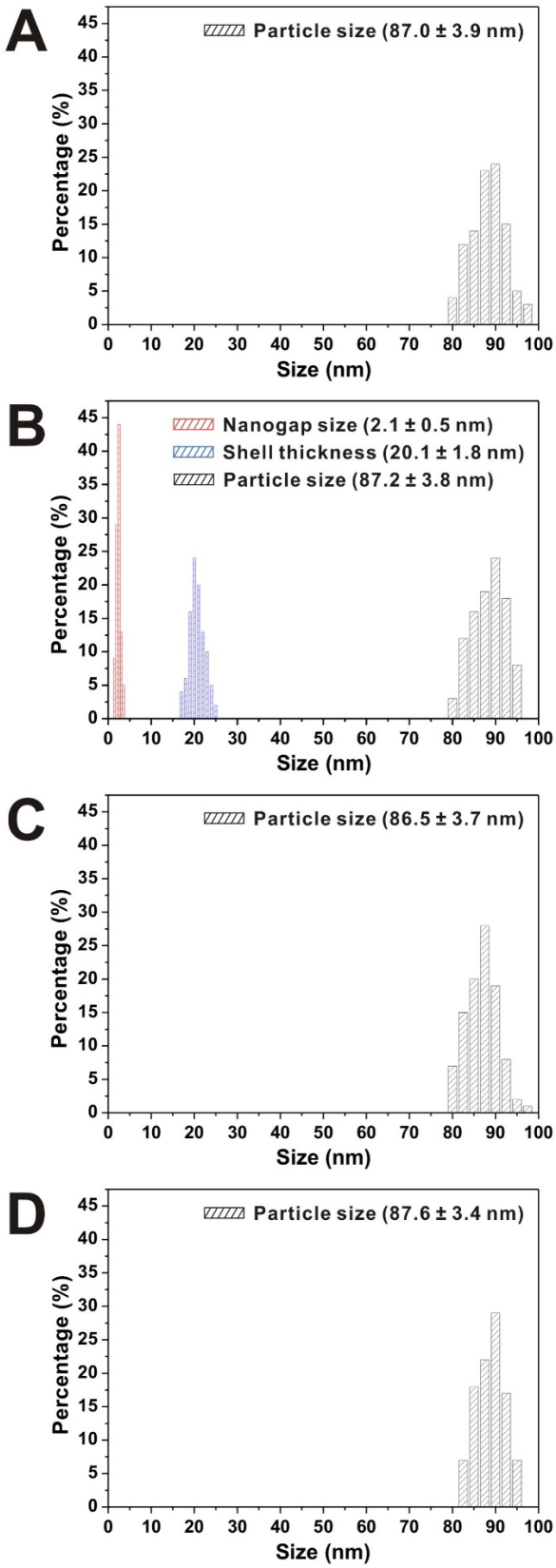

Figure S1. Interior nanogap, shell thickness, and particle size distributions of as-synthesized NPs: (A) CAS NPs, (B) DIPs, (C) gap-less AuNPs before Ag etching, and (D) gap-less AuNPs after Ag etching. Data were obtained from HR-TEM images of 100 individual particles.

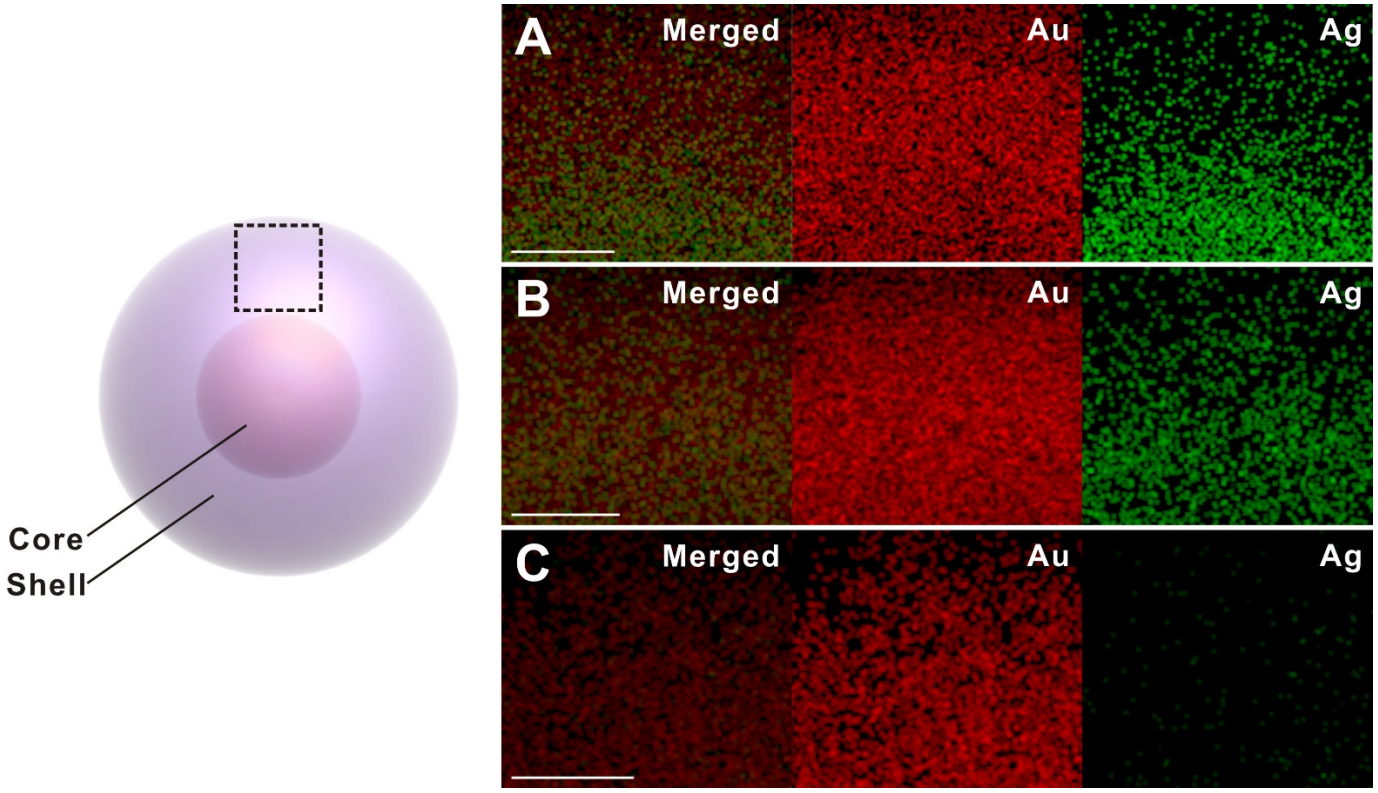

Figure S2. EDX elemental maps of as-synthesized NPs: (A) CAS NP, (B) DIP, and (C) gap-less AuNP. The maps show elemental distributions of Au and Ag in the shell region (black dotted box in left cartoon). Scale bar is 10 nm.

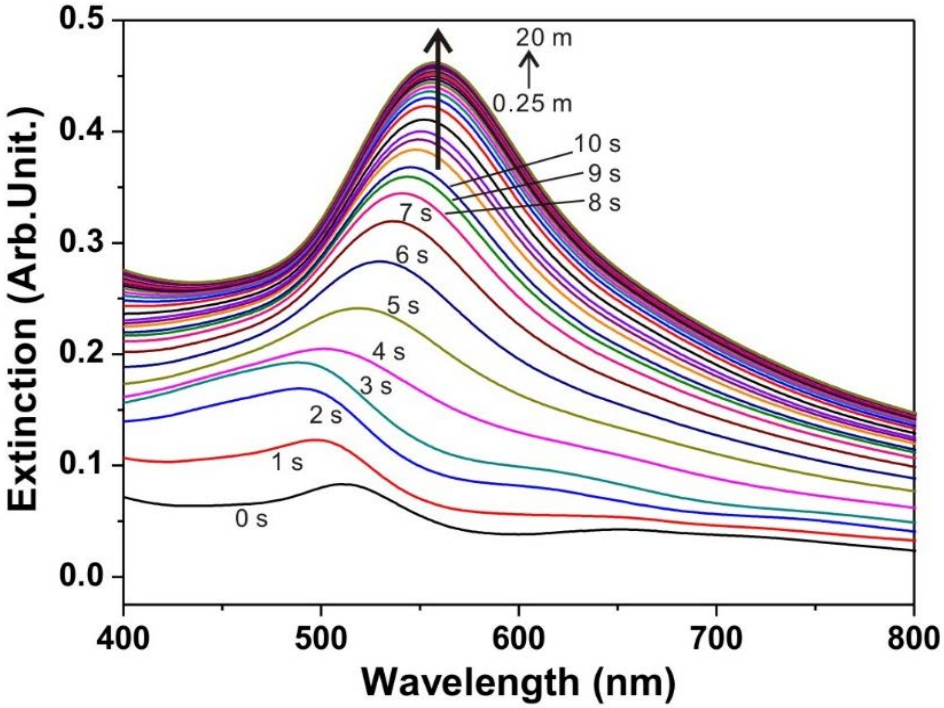

Figure S3. Changes in UV-vis spectrum of CAS NP reaction mixture during alloy shell formation.

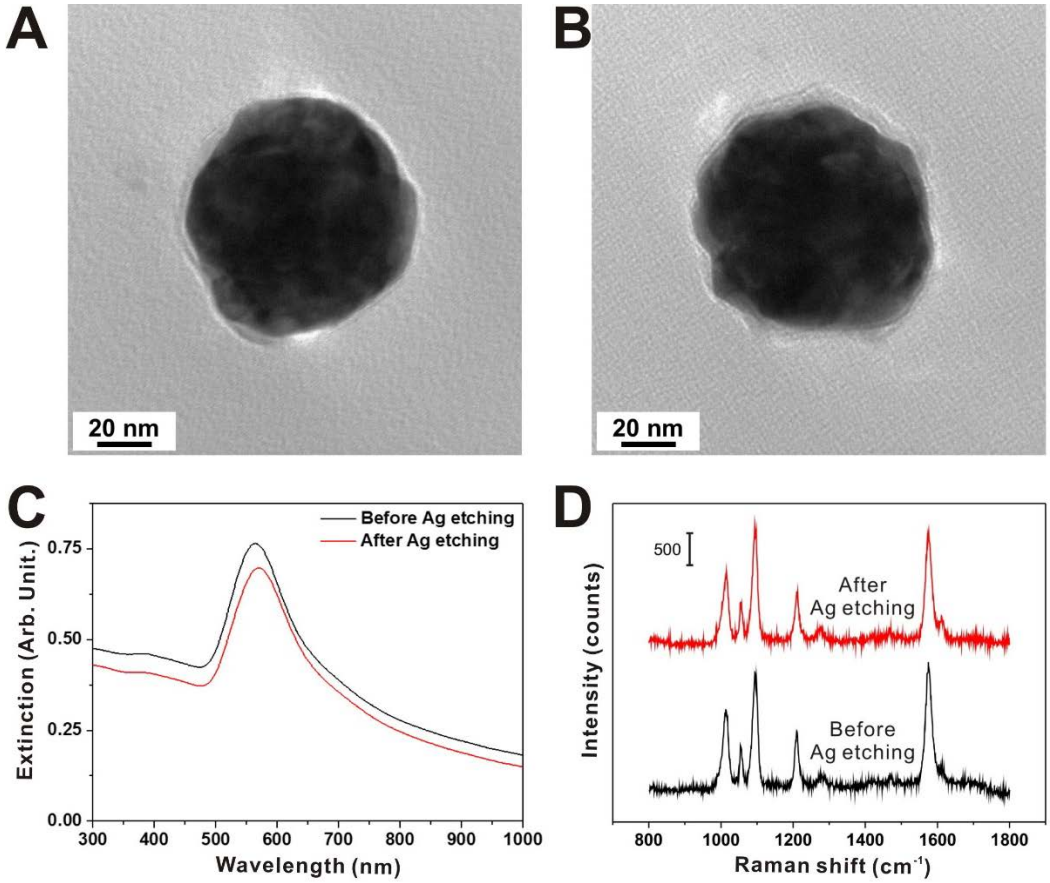

Figure S4. Structural changes and optical properties of gap-less AuNPs during Ag etching reaction. (A and B) TEM images of gap-less AuNPs: (A) before Ag etching and (B) after Ag etching. (C) UV-vis spectra of gap-less AuNPs before and after Ag etching reaction. (D) Solution-based SERS spectra of gap-less AuNPs before and after Ag etching reaction. All spectra were acquired with 633 nm laser at laser power of 4 mW and exposure time of 10 s and using same particle concentration (100 pM). The morphology, UV-vis spectra, and SERS spectra are similar, regardless of whether Ag etching reaction was performed or not, indicating that the ferric nitrate-based dealloying reaction is a Ag-specific/selective dissolution reaction.

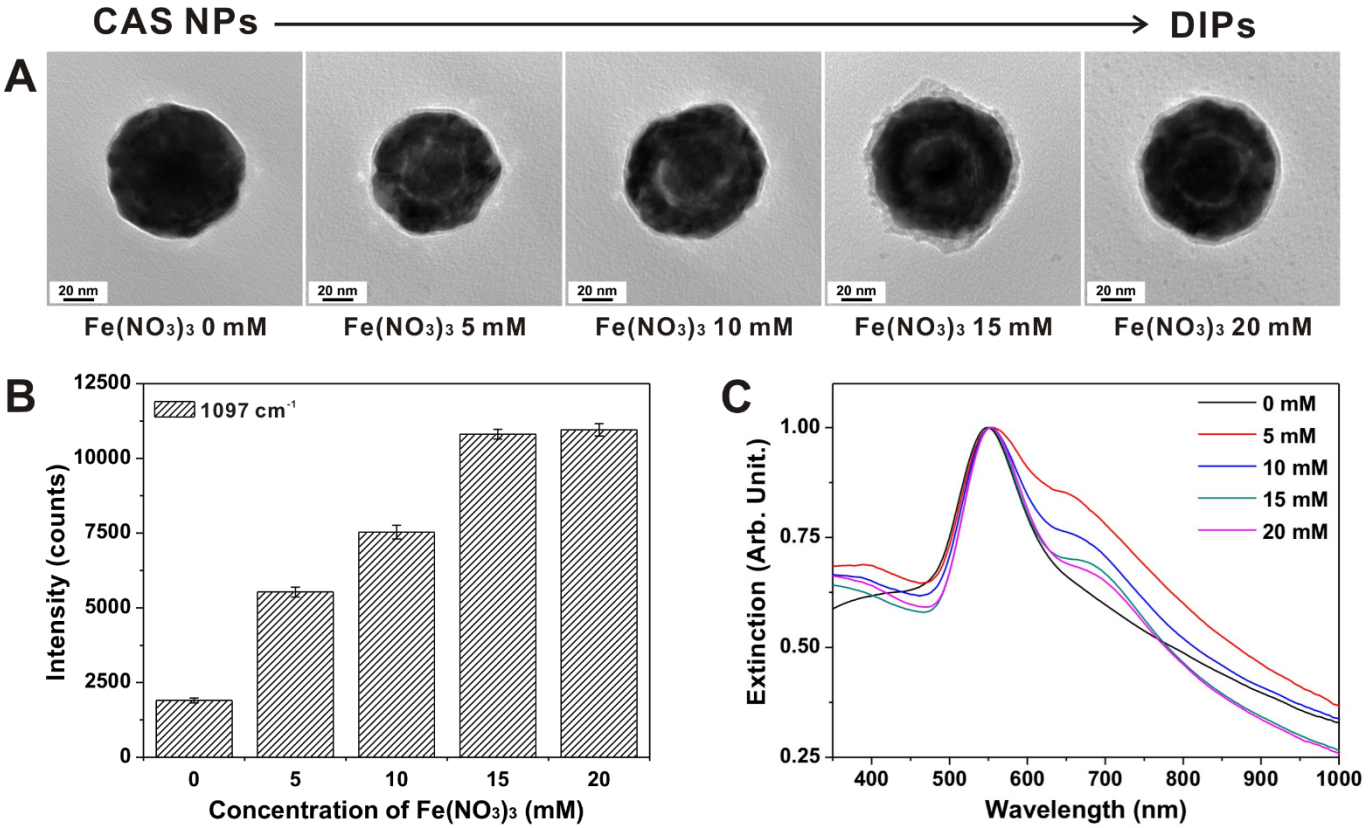

Figure S5. Changes in structure and optical properties of DIPs with dealloying reaction. (A) Structural changes in DIPs with increase in amount of $Fe(NO_3)_3$ added. The interior nanogap evolves gradually as the dealloying reaction progresses. (B) Interior-nanogap-formation-dependent changes in SERS intensity of DIPs. Solution-based SERS intensity increases with the formation of complete interior nanogap and is maximized at higher $Fe(NO_3)_3$ concentrations (more than 15 mM), indicating that the dealloying reaction is complete. SERS intensity of DIPs was nearly six times that of CAS NPs; this SERS enhancement is attributable to the strong and localized EM field generated in the interior nanogap. (C) Interior-nanogap-formation-dependent UV-vis spectra of DIPs. The extinction peaks change slightly as the dealloying reaction progresses. By the dealloying reaction, a new extinction shoulder peak appears at ~660 nm (red line), indicating the formation of the interior nanogap; this peak is slightly red-shifted to ~700 nm and is gradually stabilized after the formation of a complete and symmetric interior nanogap (purple line).

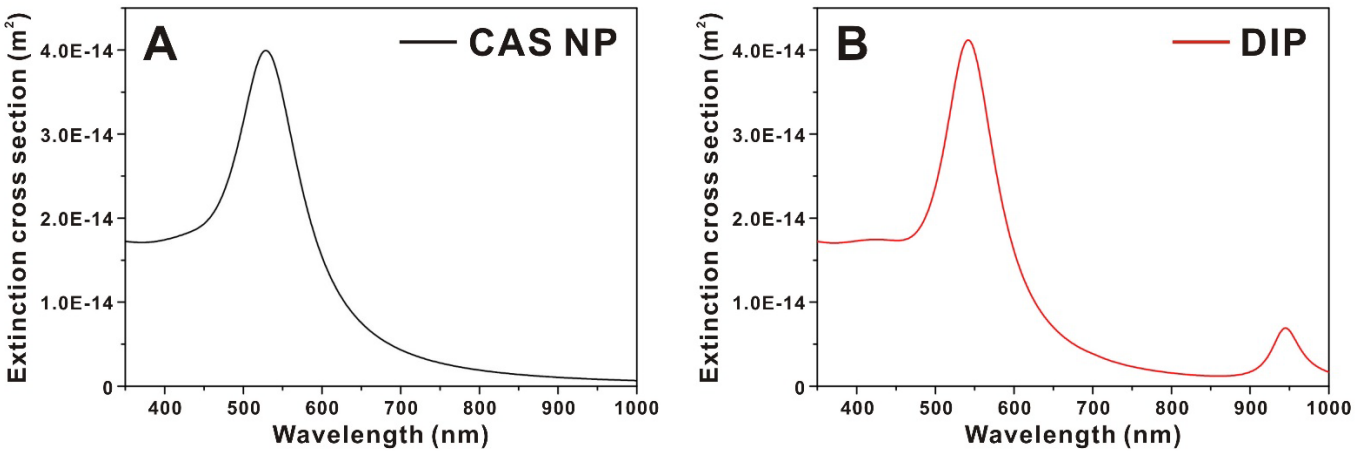

Figure S6. Simulated extinction spectra of CAS NPs and DIPs: (A) CAS NPs, (B) DIPs. The theoretical calculations were performed using Mie theory; the structural data used (average particle size, interior nanogap size, shell thickness, and atomic composition) for the as-synthesized NPs are listed in Figure S1 and Table S1. The background and interior-nanogap region were modeled as water with a refractive index of 1.33. It is worth noting that the new resonance peak at approximately 950 nm was observed only in the case of the DIPs, indicating the generation of a new plasmonic mode because of the interior nanogap.

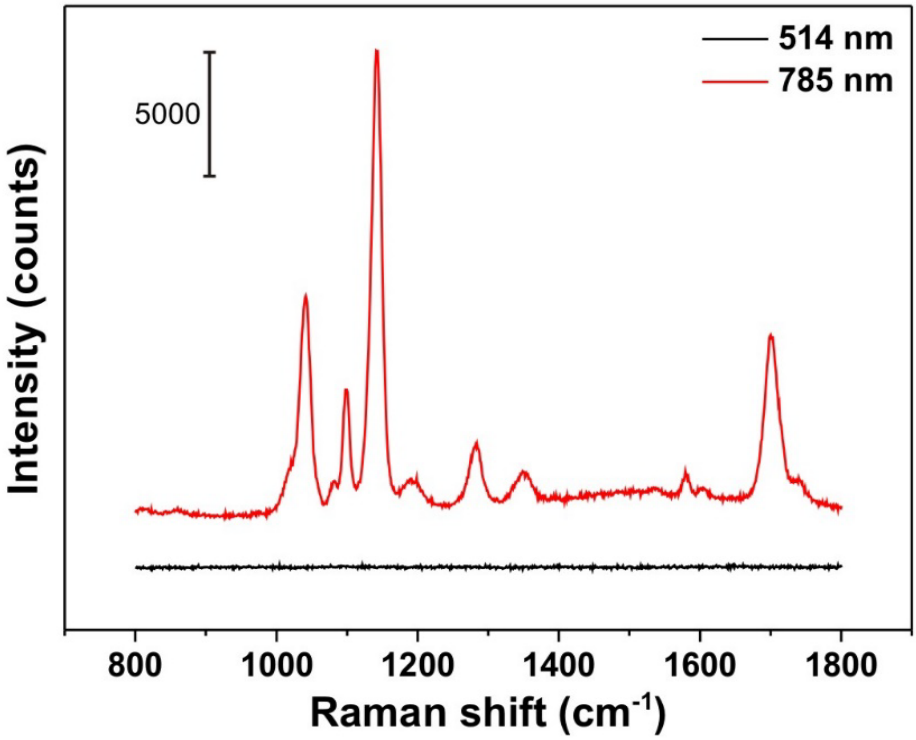

Figure S7. Excitation-wavelength-dependent SERS spectra of DIPs. The spectra were acquired using the same particle concentration (100 pM). Exposure time was 10 s and laser powers were 5 mW (514 nm) and 4 mW (785 nm).

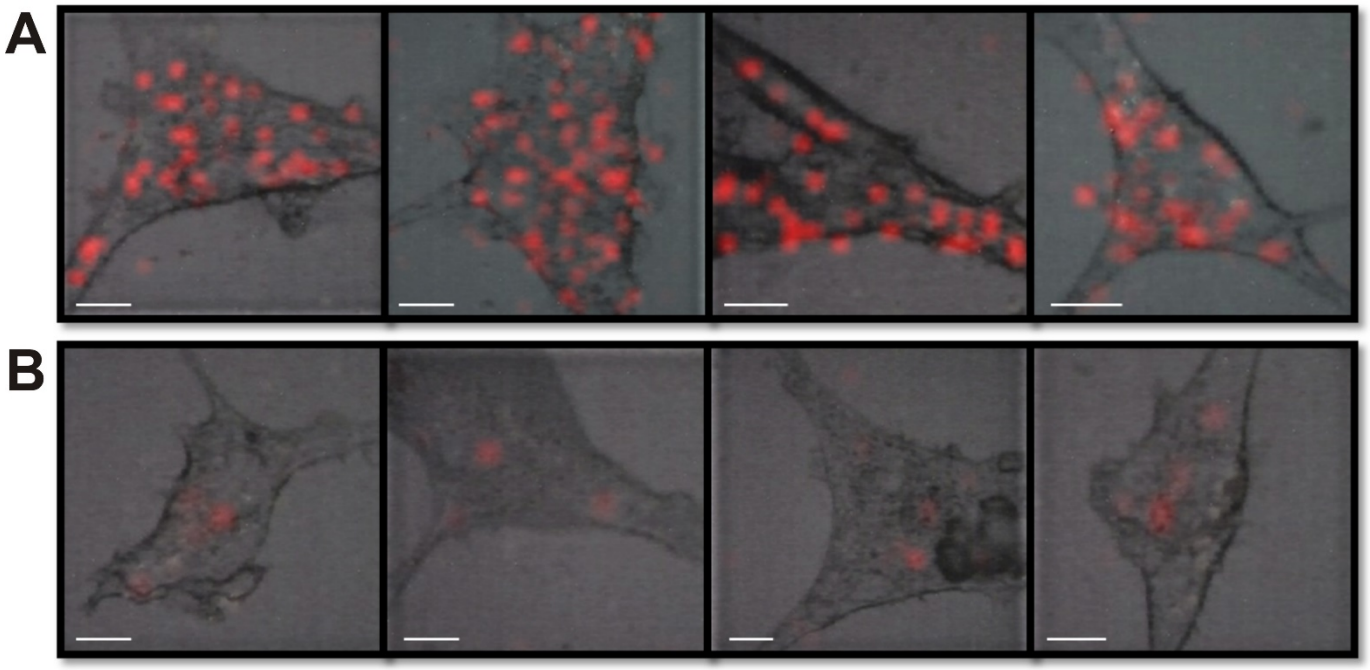

Figure S8. SERS maps of U87MG cells incubated with cRGD-functionalized imaging probes: (A) DIPs, (B) AuNPs (average diameter of 80 nm). Scale bar is 10 μm. SERS intensity at each mapping pixel (2 μm × 2 μm) was integrated for SERS spectra ranging from 983 cm^{-1} to 1023 cm^{-1} and color-scaled for cell imaging. All spectra were obtained using 633 nm excitation laser at laser power of 400 μW and acquisition time of 1 s.

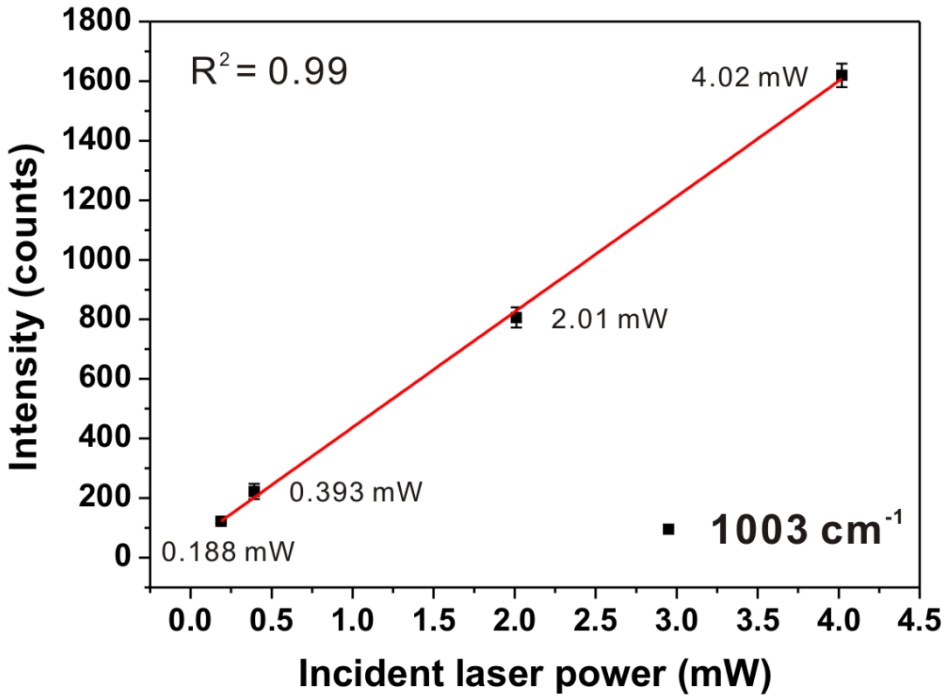

Figure S9. Incident-laser-power-dependent Raman intensities of 4-MPy solution. Raman intensity of fingerprint peak at 1003 cm^{-1} is plotted as function of incident laser power. All Raman spectra were acquired with 633 nm laser through objective lens (20×, NA = 0.4) using exposure time of 30 s. The same 4-MPy concentration (200 mM) was used for all measurements.

Table S1. Atomic compositions of shell regions of as-synthesized nanoparticles.

	Au (at%)[†]	Ag (at%)[†]
Amount of metal precursor added during synthesis[‡]	75.0	25.0
CAS NPs	77.2	22.8
DIPs	91.4	8.6
Gap-less AuNPs	100	0

[†]Atomic composition was estimated by EDX elemental mapping.

[‡]Different volumes of metal precursor (Au = 150 μL, Ag = 50 μL) were used for synthesis of alloy shell.

References

(1) Kim, M.; Ko, S. M.; Nam, J.-M. Dealloying-based facile synthesis and highly catalytic properties of Au core/porous shell nanoparticles. *Nanoscale* **2016**, *8*, 11707-11717.

(2) Lim, D.-K.; Jeon, K.-S.; Hwang, J.-H.; Kim, H.; Kwon, S.; Suh, Y. D.; Nam, J.-M. Highly uniform and reproducible surface-enhanced Raman scattering from DNA-tailorable nanoparticles with 1-nm interior gap. *Nat. Nanotechnol.* **2011**, *6*, 452-460.

(3) Lee, H.; Lee, J.-H.; Jin, S. M.; Suh, Y. D.; Nam, J.-M. Single-molecule and single-particle-based correlation studies between localized surface plasmons of dimeric nanostructures with similar to 1 nm gap and surface-enhanced Raman scattering. *Nano Lett.* **2013**, *13*, 6113-6121.

(4) Bohren, C. F.; Huffman, D. R. *Absorption and Scattering of Light By Small Particles*; Wiley: New York, 1983.

(5) Rioux, D.; Vallières, S.; Besner, S.; Muñoz, P.; Mazur, E.; Meunier, M. An analytic model for the dielectric function of Au, Ag, and their alloys. *Adv. Opt. Mater.* **2014**, *2*, 176-182.

(6) Smith, G. B. Dielectric constants for mixed media. *J. Phys. D: Appl. Phys.* **1977**, *10*, L39-L42.

(7) Song, W.; Li, W.; Cheng, Y.; Jia, H.; Zhao, G.; Zhou, Y.; Yang, B.; Xu, W.; Tian, W.; Zhao, B. Surface enhanced Raman scattering from a hierarchical substrate of micro/nanostructured silver. *J. Raman Spectrosc.* **2006**, *37*, 755-761.

(8) Song, W.; Wang, Y.; Zhao, B. Surface-enhanced Raman scattering of 4-mercaptopyridine on the surface of TiO_2 nanofibers coated with Ag nanoparticles. *J. Phys. Chem. C* **2007**, *111*, 12786-12791.